

UNCLASSIFIED

AD 276 082

*Reproduced
by the*

**ARMED SERVICES TECHNICAL INFORMATION AGENCY
ARLINGTON HALL STATION
ARLINGTON 12, VIRGINIA**



UNCLASSIFIED

NOTICE: When government or other drawings, specifications or other data are used for any purpose other than in connection with a definitely related government procurement operation, the U. S. Government thereby incurs no responsibility, nor any obligation whatsoever; and the fact that the Government may have formulated, furnished, or in any way supplied the said drawings, specifications, or other data is not to be regarded by implication or otherwise as in any manner licensing the holder or any other person or corporation, or conveying any rights or permission to manufacture, use or sell any patented invention that may in any way be related thereto.

276 082

MEMORANDUM

RM-2621-PR

MAY 1962

**DETERMINATION OF
INTERPLANETARY TRANSFER ORBITS
FOR SPECIFIED DATE OF DEPARTURE**

H. B. Schechter

PREPARED FOR:

UNITED STATES AIR FORCE PROJECT RAND

The **RAND** *Corporation*
SANTA MONICA • CALIFORNIA

MEMORANDUM

RM-2621-PR

MAY 1962

**DETERMINATION OF
INTERPLANETARY TRANSFER ORBITS
FOR SPECIFIED DATE OF DEPARTURE**

H. B. Schechter

This research is sponsored by the United States Air Force under Project RAND -- Contract No. AF 49(638)-700 — monitored by the Directorate of Development Planning, Deputy Chief of Staff, Research and Technology, Hq USAF. Views or conclusions contained in this Memorandum should not be interpreted as representing the official opinion or policy of the United States Air Force. Permission to quote from or reproduce portions of this Memorandum must be obtained from The RAND Corporation.

The RAND Corporation
1700 MAIN ST • SANTA MONICA • CALIFORNIA

PREFACE

This Memorandum, the theoretical portion of which was completed in 1960, is intended to serve as a basic aid in studies of orbital mechanics. By presenting a relatively simple and straightforward method of optimum-and nonoptimum-orbit computation, it should be of use to the engineer concerned with preliminary mission analysis. In addition, the method of solution described here has pedagogical merit because it enables beginning students of orbital mechanics to solve assignments involving three-dimensional transfer orbits, without the need for machine computations.

SUMMARY

The determination of possible interplanetary transfer trajectories for any specified date of departure, in a realistic planetary model, is a complex problem which requires the use of high-speed computers. Reference 2 presents some of the solutions obtained for the case of Martian transfers.

For purposes of preliminary design and mission planning it would be useful to be able to compute some realistic transfer curves without extensive machine runs.

This Memorandum presents a method of solution which enables one to determine arbitrary transfer orbits quickly and accurately using only a desk computer.

Coplanar, as well as three-dimensional, surface-to-surface trips were investigated, and account was taken of the eccentric shape of the planetary orbits.

A number of transfer orbits from Earth to Mars were computed for two arbitrarily selected dates of departure. The numerical results are summarized in a series of curves which display the characteristic velocity expenditures for trips of various durations, as well as the orientation of the departure velocity vector.

In the case of three-dimensional transfers, two separate regions of minimal characteristic velocity are found. The two regions are separated by a narrow belt corresponding to transfer angles in the vicinity of 180 deg. Within this zone of separation, which corresponds to departures at right angles to the ecliptic, transfer velocities rise sharply.

CONTENTS

PREFACE	iii
SUMMARY	v
LIST OF SYMBOLS	ix
Section	
I. INTRODUCTION	1
II. GEOMETRIC PROPERTIES	4
III. COPLANAR TRANSFERS BETWEEN CIRCULAR ORBITS	13
IV. THREE-DIMENSIONAL TRANSFERS WITH ECCENTRICITY	24
Appendix	
A. NUMERICAL EXAMPLE	35
B. CHARACTERISTIC TRANSFER VELOCITY IN THREE DIMENSIONS	41
REFERENCES	45

SYMBOLS*

A , a = semimajor axis of elliptic orbit

A_e , A_m , A_o = specific values of the semimajor axis, as defined in Eq. (3)

C , c = chord joining departure point P to destination point Q

e = eccentricity of elliptic orbit

F = active focus, or function defined by Eq. (10)

F^* = vacant focus located on L_+ branch of Fig. 2

\tilde{F}^* = vacant focus located on L_- branch of Fig. 2

g = function defined by Eq. (9)

i = included angle between planetary orbital planes

L , ℓ = semilatus rectum

M = mean anomaly of destination planet

M_1 , M_2 = values of mean anomaly at departure and arrival, respectively

N_A , N_D = ascending and descending nodal axes

N_M = mean angular velocity of Mars (N.D.)

n = number of complete revolutions of transfer vehicle

P = designation of departure point

Q = designation of arrival point

R_E , R_M = mean radii of planets Earth and Mars, respectively

r = radial distance from Sun

r_1 , r_2 = mean radii of initial and terminal planetary orbits

s , S = parameter defined after Eqs. (1)

* In the following, whenever a letter symbol appears as both capital and lower-case (e.g., A , a), the capital refers to nondimensionalized quantities. In all other instances, nondimensional parameters will be indicated by (N.D.).

t = time
 τ = time (N.D.)
 τ_0 = time taken by Mars to cover prescribed arc (N.D.)
 V, v = velocity
 v_{CH}, v_{CR} = characteristic velocity
 v_{CH_1}, v_{CR_2} = characteristic velocity components at departure and arrival
 α, β = parameters defined after Eqs. (1)
 γ_1 = angle subtended by ecliptic component of departure velocity vector with Earth's orbit
 δ = angle subtended by departure velocity with ecliptic plane
 ϵ = angle included between transfer and destination planes
 θ = transfer angle
 θ_0 = initial longitude difference of planets (two-dimensional)
 λ = constant Lagrange multiplier
 μ = solar gravitational constant
 ν = true anomaly
 ρ = radial distance from Sun (N.D.)
 ρ_2 = mean radius of Martian orbit
 ρ_M = radial distance corresponding to an anomaly M
 ϕ = final position of Mars from ascending nodal axis N_A
 $\Delta\phi$ = angle traversed by Mars, as given in Eq. (4)
 ϕ_1 = initial position of Mars
 ξ = location of Mars' perihelion, as shown in Fig. 7
 ω = position of Earth at departure
 ω_M = mean angular velocity of Mars

SUBSCRIPTS

a = aphelion

CH = characteristic

E, M = Earth and Mars, respectively

i = initial

PQ = movement on transfer ellipse from point P to point Q

p = perihelion

r, θ = radial and transverse directions in Martian plane

X = refers to any one of the subscripts F, F^* , or FF^* ,
depending on circumstances

I. INTRODUCTION

During the planning stage of any interplanetary-transfer mission, there exists, for purposes of preliminary design, a very distinct need for quick and reliable information concerning the merits of the various transfer orbits which can be selected to accomplish the given mission.

Two of the main items of interest during this stage of the investigation are the time of flight and the so-called characteristic velocity of transfer.

Time, obviously, is of great importance if one considers manned space missions, since it affects directly the crew requirements for the duration of the trip.

The characteristic velocity, on the other hand, affects the propellant requirements, and thus the size of the final vehicle. The influence on vehicle size decreases markedly as one progresses to the use of fuels having a very high specific impulse.

In the initial stages of interplanetary flight analysis, mission-cost and flight-time estimates between coplanar, concentric circular planetary orbits were obtained by the application of the concept of cotangential transfer orbits, also known as Hohmann ellipses. Although these transfer orbits led to low values of the characteristic transfer velocity, they required relatively long transfer times. In addition, the use of these orbits presupposes a propitious location of the two planets at departure, a condition seldom encountered in practice.

Cotangential ellipses cease to exist in a three-dimensional model of the planetary system, irrespective of whether the planetary orbits are still considered to be circular or elliptic. Even so, this concept can still find an

occasional application for those instances when the target planet happens to cross the nodal axis at the time of intercept, and the departure point is situated 180° away.

With the exception of these special cases, transfer orbits will lie in planes of arbitrary, though determinable, orientations in space, depending on the departure date selected and the time available to transit. The simple back-of-the-envelope type of trajectory computations for the two-dimensional circular planetary model that were introduced by the early investigations in the field were replaced by complicated coding routines for high-speed digital computers, into which the exact orbital positions of the planets could be fed.

This Memorandum presents a method which allows one to determine and compute with relative ease any type of two-impulse transfer trajectory, in two and three dimensions, for a given date of departure if the time available for the flight is specified in advance. Since only elliptic transfer orbits have been considered here, this implies that among all the possible ellipses which pass through the given initial point, and specified final point, only that ellipse is isolated which enables the vehicle to spend the pre-selected number of days in transit. Moreover, this calculation can be carried out in a very short period of time (2 to 3 hours) on a regular desk computer without the use of high-speed digital machines. In addition, it is shown how the formalism of some of the theorems of the calculus of ordinary maxima and minima facilitates the location of those trajectories which, for a given departure date, require the least expenditure of characteristic velocity of transfer.

In Ref. 1, Battin introduced a very convenient geometric formulation in

the two-dimensional portion of his work, in which he treated transfers between arbitrary points on circular planetary orbits. The necessary initial locations of the planets were then computed as soon as an optimal trajectory was found. The same geometric parameters will be retained here.

Starting out with a two-dimensional problem, we introduce a subsidiary intercept constraint condition on the transfer orbit which enables one to calculate transfers directly for only those planetary configurations at departure which are of current interest. The formalism of the optimality condition for the present case, analogous to the one developed by Battin, is somewhat more complicated because of the need to introduce Lagrange multipliers.

The same basic approach is then extended to solve the case where the destination orbit is elliptic in shape, and it is eventually applied to the more realistic model in which the orbital planes of the planets are mutually inclined to each other.

The difficulties introduced by the inclusion of orbital eccentricity have been overcome by retaining in the series expansions of the planetary orbital elements only first-order terms in eccentricity. The very small values of this quantity for the orbits of Earth and Mars justify this approximation.

The numerical results of the present investigation were compared with those of Ref. 2 and, to the order of accuracy of the data presented there, were found to be in good agreement with them.

II. GEOMETRIC PROPERTIES

The geometrical relationships which will be of use in the subsequent development will be stated here without proof. Those interested in the derivations are referred to Ref. 1. Distances, velocities, and times are non-dimensionalized with respect to the astronomical unit; Earth's mean speed around the sun, $\sqrt{\frac{\mu}{r_1}}$; and its mean angular velocity $\sqrt{\frac{\mu}{r_1^3}}$, respectively.

For that part of the calculations in which the orbits of both Earth and Mars were assumed to be circular, a transfer from a point P on the orbit of the first planet to a point Q on the orbit of the second planet would take place between the radial distances r_1 and r_2 of the transfer ellipse. Only direct transfer orbits were considered here because of their lower cost.

For a prescribed angle θ between the above two radii, the time of transit will depend on both the magnitude and the orientation of the semimajor axis of the transfer ellipse. The time can be calculated from Lambert's theorem, a derivation of which can be found in Ref. 3. Denoting by F the active focus of the transfer ellipse at which the Sun is located, and by F^* the vacant focus, we can distinguish among four possible modes of transfer from P to Q, as indicated in Fig. 1.

Which one of the following relations for the time of travel will be used at any one instance will depend on whether the contour from P to Q and back to P via the chord QP, traversed in a counterclockwise direction, does or does not enclose one or both of the focal points F and F^* .

The sense of the motion will be taken as positive in the counterclockwise direction.

The various expressions for the dimensionless time of transit can then

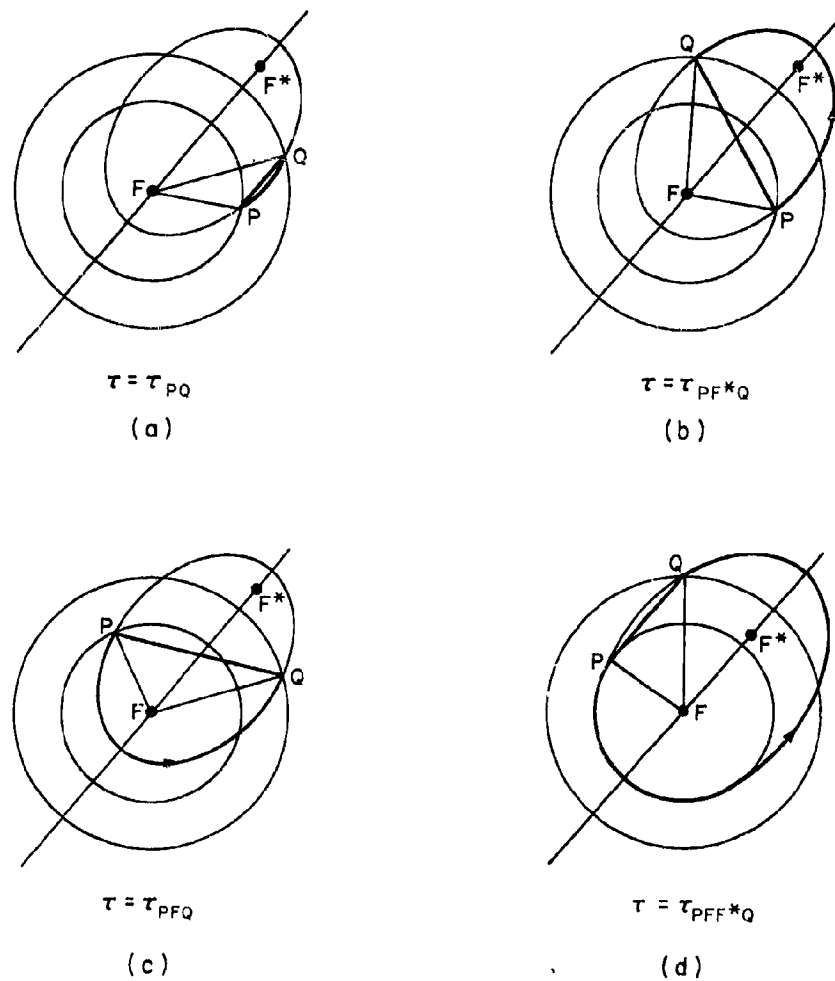


Fig.1—Possible transfer ellipses

be written as follows:

$$\tau_{PQ} = A^{3/2} \left[(\alpha - \sin \alpha) - (\beta - \sin \beta) \right] \quad (1a)$$

$$\tau_{PF^*Q} = 2\pi A^{3/2} - A^{3/2} \left[(\alpha - \sin \alpha) + (\beta - \sin \beta) \right] \quad (1b)$$

$$\tau_{PFQ} = A^{3/2} \left[(\alpha - \sin \alpha) + (\beta - \sin \beta) \right] \quad (1c)$$

$$\tau_{PFF^*Q} = 2\pi A^{3/2} - \tau_{PQ} \quad (1d)$$

where the angles α and β are given by the relations

$$\sin \frac{\alpha}{2} = \sqrt{\frac{s}{2a}}$$

$$\sin \frac{\beta}{2} = \sqrt{\frac{s-c}{2a}}$$

$$2a = r_1 + r_2 + c$$

$$\tau = t \sqrt{\frac{\mu}{r_1^3}}$$

$$A = \frac{a}{r_1}$$

$$\beta < \alpha < \pi$$

Expression (1a) is used when the contour does not enclose either one of the foci, as in (a) of Fig. 1. When PQP encloses the vacant focus F^* , as in (b) of Fig. 1, one uses Expression (1b). If, on the other hand, the active focus is enclosed, as in (c) of Fig. 1, one uses Expression (1c). When both F and F^* are situated within the contour PQP , as in (d) of Fig. 1, one must apply Expression (1d).

Another useful parameter is the semilatus rectum L of the transfer orbit.

In its most familiar form, it is expressed as

$$L = A(1 - e^2) = \frac{4A(S - 1)(S - \rho_p)}{c^2} \sin^2 \frac{\alpha \pm \beta}{2} \quad \text{ellipse} \quad (2a)$$

$$= 2\rho_p \quad \text{parabola} \quad (2b)$$

$$= A(e^2 - 1) = \frac{4A(S - 1)(S - \rho_p)}{c^2} \sinh^2 \frac{\alpha \pm \beta}{2} \quad \text{hyperbola} \quad (2c)$$

where ρ_p = perifocal radius, and the angles α and β are functions of $\frac{r_1 + r_2}{r_1}$ and c .

For those cases where the time of transit did not have to satisfy a constraint condition, the selection of the positive sign in the expression for the semilatus rectum L led to lower values of the characteristics transfer velocity. This can be shown by plotting V_{CH} vs A , and it is found to hold true for all values of the transfer angle θ . Now that the transfer time has a constraint imposed on it, it can be shown that not all the dates considered for departure allow one to follow an elliptic path with L_+ . To ensure the existence of elliptic transfer orbits for all the possible initial positions of the planets, and to minimize the number of complete orbital revolutions before arrival, both values of the quantity L are retained in the analysis.

One further point worth mentioning concerns the orientation of the transfer ellipse. For given values of r_1 , r_2 , and included angle θ , this orientation depends on the magnitude of the semimajor axis, as well as on the position of the vacant focus F^* with respect to the chord C joining P and Q . The choice of the sign in the expression for the semilatus rectum serves to determine on which side of the chord C the focus F^* will be located. Figure 2,

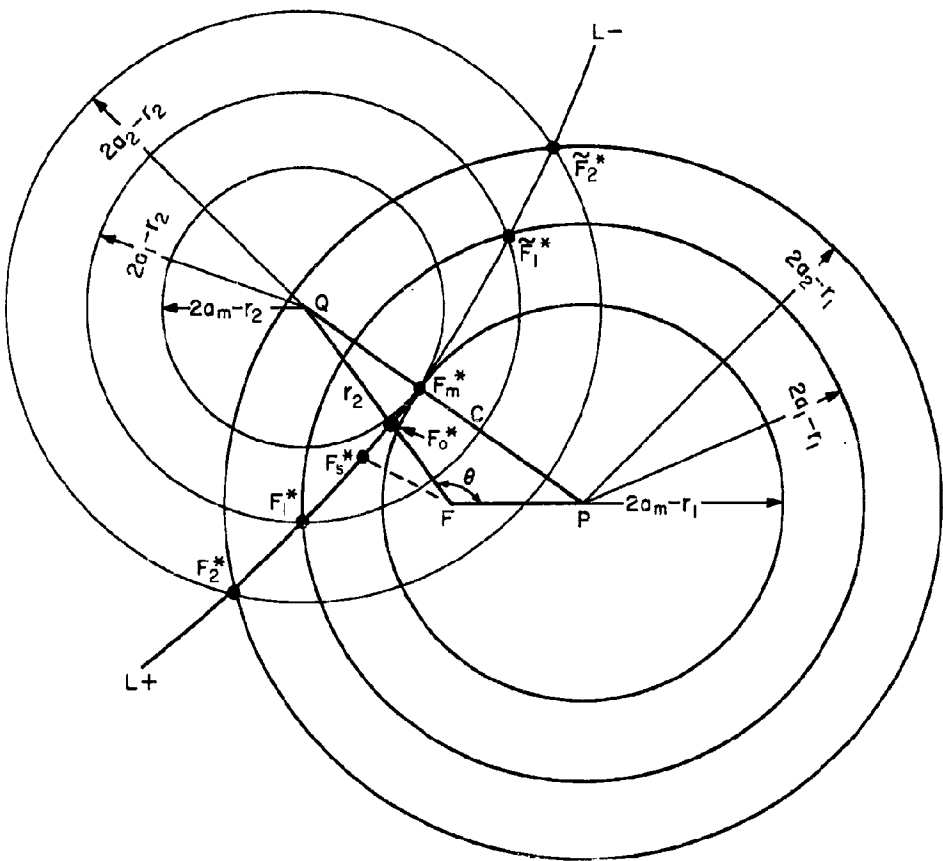


Fig.2—Locus of the vacant foci for elliptical trajectories

which is similar to Figs. 1 - 4 of Ref. 1, indicates the locus of possible F^* positions, with the heavy branch of the curve denoting the region of L_+ . This curve turns out to be a hyperbole. If a particular position of F^* is chosen, the orientation of the major axis of the transfer ellipse is then found by joining the points F and F^* . Depending on the orientation of this axis, a vehicle leaving point P along a suitable transfer orbit would reach point Q either before or after passing an apse of the transfer ellipse.

Referring to Fig. 2, a few critical points located on the curve determined by the loci of F^* can be noticed. The point F_m^* is the vacant focus of the ellipse with the minimum semimajor axis; F_o^* is the vacant focus of the transfer ellipse with aphelion located at point Q . For values of $\frac{\pi}{2} < \theta < \pi$ a third point of interest is F_1^* which defines the ellipse with perihelion at P . With each of these vacant foci there is associated a magnitude of the semimajor axis of the transfer ellipse. Denoting these respective parameters by A_m , A_o , and A_ℓ , where

$$A_m = \frac{r_1 + r_2 + c}{4r_1}$$

$$A_o = \frac{r_2/r_1}{1 + \frac{r_2 - r_1}{r_2 - r_1 \cos \theta}} \quad (3)$$

$$A_\ell = \frac{r_1 - r_2 \cos \theta}{2r_1 - r_2(1 + \cos \theta)} \quad \frac{\pi}{2} \leq \theta \leq \frac{3\pi}{2}$$

and

$$A_\ell > A_o > A_m$$

we can determine the orientation of the transfer ellipse from P to Q simply from a knowledge of the magnitude of its semimajor axis A.

The dependence of travel time τ on semimajor axis A of the transfer ellipse is indicated in Fig. 3 for two arbitrary values of the transfer angle θ .

Turning our attention for the moment back to Fig. 2, we observe that for a given value of θ , the junction of the two branches of the loci of F^* occurs at a value of $A = A_{\min}$. The same behavior is also exhibited in the τ vs A graph of Fig. 3.

From Fig. 2, which happens to be drawn for $\theta > \frac{\pi}{2}$, we note that as $A \rightarrow \infty$, the direction of the major axis, or the line joining F and F^* on the L_+ branch, becomes parallel to the asymptote of the hyperbola of F^* . This places the perifocal apse on the segment of arc joining P and Q. Since this region implies high orbital velocities, it is reasonable to assume that transfer times along this arc are going to be of short duration. This expectation is borne out by the L_+ branch of the $\theta = 60$ deg curve of Fig. 3. (The fact that here $\theta < \frac{\pi}{2}$ will not alter the conclusions reached before, except for the fact that now the perifocal apse will be located slightly ahead of the point P, rather than between P and Q. Point P will still have high orbital velocities associated with it.) As the point F^* slides along the L_+ branch of the hyperbola in the direction of decreasing A, the transfer ellipses rotate in a clockwise direction, thereby moving the perifocal apse away from point P. The attendant lower orbital velocities in the region between P and Q will result in an increase in travel time τ , as exemplified by the lower branch of the $\theta = 60$ deg curve. The largest available value of τ along this branch will occur when a value of $A = A_{\min}$ is reached. If

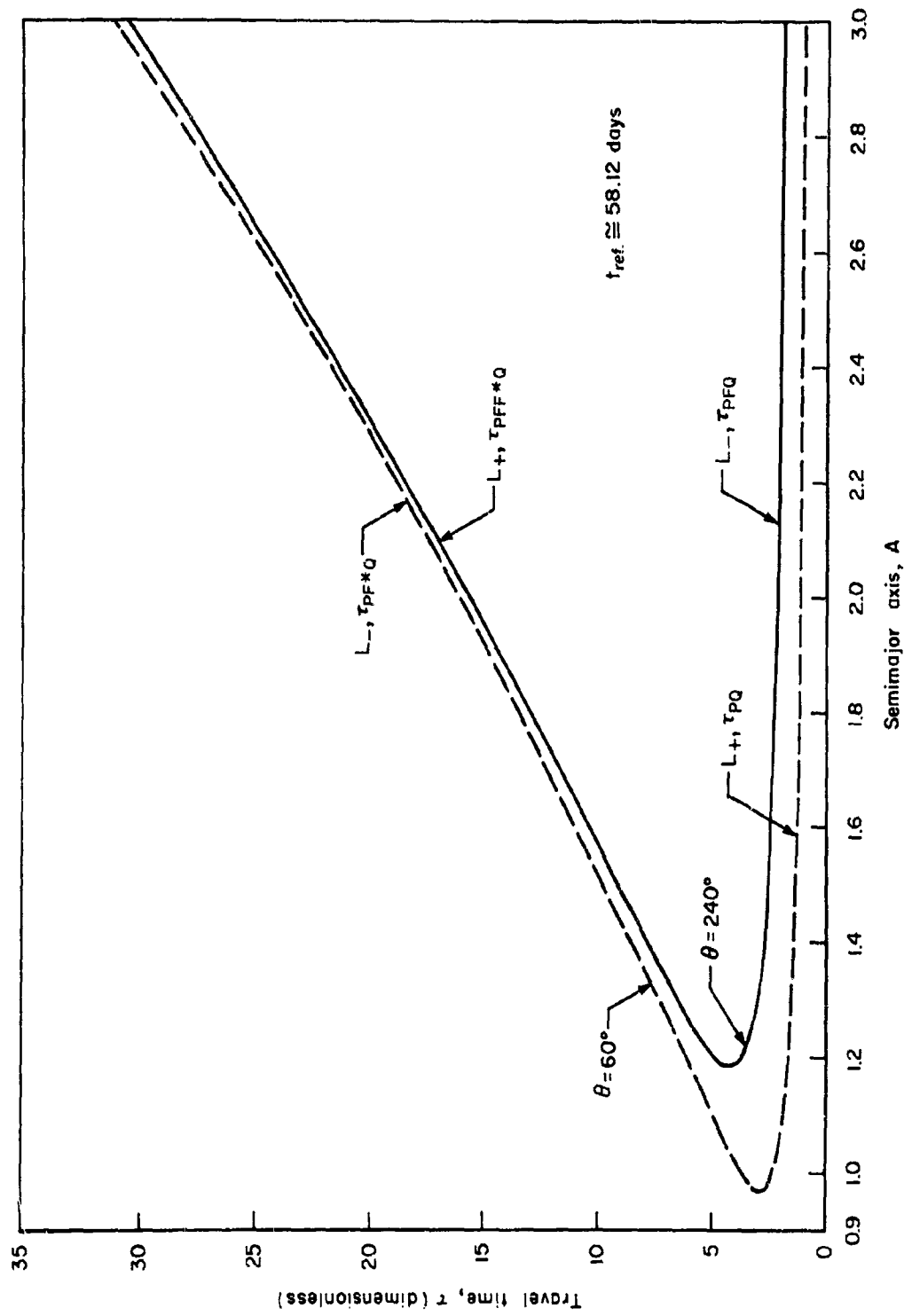


Fig. 3—Variation of transfer time with semimajor axis

longer travel times are desired, the vacant focus F^* will have to continue to slide out into the F^* region ($L = L_-$), thereby causing the vehicle to move past a more remote apofocal point, and consequently into a region of ever-diminishing orbital velocities. The lower orbital velocities coupled with the longer distances that have to be traversed as A keeps on increasing will lead to longer transfer times, as shown in the upper branch (L_-) of the $\theta = 60$ deg curve of Fig. 3.

For values of $\theta > \pi$, the L_+ and L_- branches of the hyperbola become reversed, thus explaining the $\theta = 240$ deg curve of Fig. 3.

An examination of the equations presented in this section discloses the fact that for transfers between circular orbits where r_1 and r_2 are constants, the time τ as well as the semilatus rectum L depends only on the semimajor axis A and the chord C between points P and Q .

III. COPLANAR TRANSFERS BETWEEN CIRCULAR ORBITS

Before looking at the more general and realistic case of transfers in three dimensions between elliptic orbits, it is advantageous to start out by considering at first the simpler case of transfer from the surface of the Earth to the surface of Mars, assuming that both planets describe circular coplanar orbits about the Sun. With some obvious minor modifications, the same analysis would apply also to transfers to inner planets, such as from Earth to Venus, or to the return trip from Mars to Earth.

It will be assumed that the mission is accomplished by the application of two impulsive thrusts at both terminals of the transfer curve. The first thrust enables the vehicle to escape the Earth's gravitational field and leaves it with a hyperbolic excess velocity of a magnitude and direction such as to place it into heliocentric elliptic intercept orbit. The second impulse is employed both to cancel the relative velocity of the vehicle with respect to Mars, on its arrival there along the chosen heliocentric collision course, and to overcome the gravitational attraction of that planet. This will permit the vehicle to make a soft landing on Mars. The assumed scheme of transfer does not make any allowances for the various losses (gravitational, atmospheric, navigational, etc.) that arise in an actual space mission nor for possible gains from atmospheric braking on re-entry. Nonetheless, the present method will be well suited to assess the rough over-all costs of such a transfer and to give an idea of the correlation between launch date and total velocity requirement. To hold the needed characteristic velocities down to a reasonable level, transfers along elliptic orbits only will be investigated. The modifications needed to include faster transfers will affect primarily the expressions for time of transfer and semilatus rectum.

The complete surface-to-surface transfer trajectory was assumed to be composed of three discrete segments, each segment being generated as a result of a two-body interaction.

The junction of the heliocentric portion of the orbit with the planetocentric segments at departure and arrival was assumed to occur along the asymptotes to the planetocentric hyperbolae. At each end, the planetary influence on the terminal portion of the trajectory was assumed to be concentrated in an imposition of the appropriate escape velocity requirement, which was added vectorially to the planetocentric hyperbolic excess velocity.

The major benefit which the present approach brings to the three-dimensional case is the ability to solve for any one transfer trajectory, given the positions of the two planets at departure.

Consider the physical picture where the two planets occupy specified positions along their orbits on the specific date chosen for launch from the Earth. In the two-dimensional restricted case, only the angle between the orbital radii of the two planets suffices to specify their relative position at departure, their actual positions in their respective orbits being immaterial.

After the initial impulse is imparted to the vehicle, it will find itself with a certain initial velocity vector, in a heliocentric frame of reference. This velocity is already assumed to include the contribution from the circumferential velocity of the Earth in its path around the Sun.

The two components of this departure velocity vector, in the radial and transverse directions, suffice to specify completely the geometrical parameters of the transfer ellipse. Starting out with the above conditions at point P, and following the selected orbit, the vehicle will intersect the

orbit of Mars at some future time, at some point Q. Since this crossing must occur at the precise moment when Mars happens to pass the same spot, it becomes necessary to restrict the domain of possible departure conditions. A sufficient restriction on the departure conditions results if one demands that the time of travel from P to Q, along the transfer orbit, be the same as the time required by Mars to reach the same terminal point Q. If one associates with each time of transfer, defined by the appropriate equality in Eqs. (1), a transfer angle θ included between the radii $r_1 = r_P$ and $r_2 = r_Q$ and remembers that in the present case Mars moves with a constant angular velocity, one can then write

$$\Delta\theta = \theta - \theta_0 - 2\pi n \quad (4)$$

where

$$\Delta\theta = \frac{v_M}{r_2} t = \text{angle traversed by Mars during time } t$$

θ_0 = lead angle of Mars at departure

v_M = dimensional circumferential velocity of Mars

$n = 0, 1, 2, 3$ = number of revolutions around the Sun completed by the vehicle

For the selection of optimal transfer curves, the procedure of optimization then consists of hunting among the various acceptable points Q for that particular point which permits the mission to be accomplished with a minimum expenditure of total characteristic velocity. This hunting can be performed automatically by means of a high-speed computer, or manually on a desk calculator.

Another possible way of viewing the problem is the one in which we search for that particular transfer ellipse which requires the vehicle to spend a period of time in orbit of such length that both the requirement of minimal characteristic velocity and the restraint imposed by Eq. (4) are satisfied simultaneously.

With the above physical picture in mind, it is easy to appreciate the mathematical formulation which leads to the required solution.

The quantity to be minimized in the present case is the total characteristic velocity of the one-way landing mission, given in nondimensional form by

$$v_{CH} = \left\{ 3 = \frac{1}{A} - 2\sqrt{L + K_3} \right\}^{1/2} + \frac{1}{\sqrt{\rho_2}} \left\{ 3 = \frac{\rho_2}{A} - 2\sqrt{\frac{1}{\rho_2} + \rho_2 K_4} \right\}^{1/2} \quad (5)$$

$K_3 = \frac{2\mu_E}{\mu} \frac{r_1}{R_E}$ = square of dimensionless escape velocity at Earth

$K_4 = \frac{2\mu_M}{\mu} \frac{r_1}{R_M}$ = square of dimensionless escape velocity at Mars

The first term of Eq. (5) was the one derived in Ref. 1 for a nonattracting Earth ($K_3 = 0$).

The chord joining points P and Q can be expressed in terms of the angle θ by means of

$$c^2 = 1 + \rho_2^2 - 2\rho_2 \cos \theta \quad (6)$$

where the angle θ depends on the time of travel of Mars, τ_0 , through the relation

$$\theta = 2\pi n = \theta_0 + N_M \tau_0 \quad (7)$$

In the above equation, $N_M = \omega_M \sqrt{r_1^3/\mu}$ is the dimensionless mean angular velocity of Mars, and ω_M is the corresponding dimensional angular velocity. The reference time, $\sqrt{r_1^3/\mu}$, is 58.12 days.

The selection of a departure date fixes immediately the value of the angle θ_o . In order to make contact with Mars on arrival, one has to require that the time of travel in the transfer orbit, τ , given by the appropriate expression in Eqs. (1), should equal the time τ_o taken by Mars to reach the same spot, for every value of the angle θ_o .

Thus

$$\tau = \tau_o \quad (8)$$

is a required condition on the transfer orbit. Noting that by means of Eqs. (6) and (7) the time $\tau_o = \tau_o(\theta_o, C)$, and that from Eqs. (1) the time $\tau = \tau(A, C)$, one can write Condition (8) in the form

$$g(A, C, \theta_o) = \tau - \tau_o = 0 \quad (9)$$

Our optimization problem now takes the following form.

It is desired to minimize the function $V_{CH} = V_{CH}(A, C)$ given in Eq. (5), subject to the subsidiary condition of Eq. (9). In accordance with standard procedures of the calculus of maxima and minima, this entails the determination of an extremal value of a function F , given by

$$F = V_{CH} + \lambda g \quad (10)$$

where λ is a constant Lagrange multiplier. The extremals are obtained upon setting

$$\frac{\partial F}{\partial A} = \frac{\partial F}{\partial C} = \frac{\partial F}{\partial \lambda} = 0 \quad (11)$$

The relation

$$\frac{\partial F}{\partial C} = \frac{\partial V_{CH}}{\partial C} + \lambda \frac{\partial g}{\partial C} = 0$$

can be used to solve for λ , which can then be substituted in the equation $\frac{\partial F}{\partial A} = 0$. When this is done, the condition for an extremal in V_{CH} becomes

$$T(A, C) = \frac{\partial V_{CH}}{\partial A} - \frac{\frac{\partial V_{CH}}{\partial C}}{\frac{\partial g}{\partial C}} \frac{\partial g}{\partial A} = 0 \quad (12)$$

in addition to Eq. (9).

A suitable method for computing optimal trajectories would consist of the following steps:

- a. For a particular date of departure the angle θ_0 is a known quantity, available from astronomical tables. The angular positions of Earth and Mars, reckoned from the ascending nodal line, are presented in Fig. 4. In the case of circular orbits, both curves become straight lines of known slope. These lines intersected on January 1, 1961, at which time Mars was in opposition to the Earth.
- b. A guess for a reasonable value of transfer angle θ allows one to compute C and τ_0 by means of Eqs. (6) and (7), respectively.
- c. In view of Eq. (9), Eq. (1) can then be solved for a value of the semimajor axis A . This step will in general involve an iteration procedure for A , which converges rather rapidly.
- d. The values of A and C found from steps (b) and (c) above are then placed into Eq. (12), and the value of $T(A, C)$ is compared with zero.
- e. The procedure is repeated, starting out with a slightly changed value of θ , while keeping θ_0 unchanged.

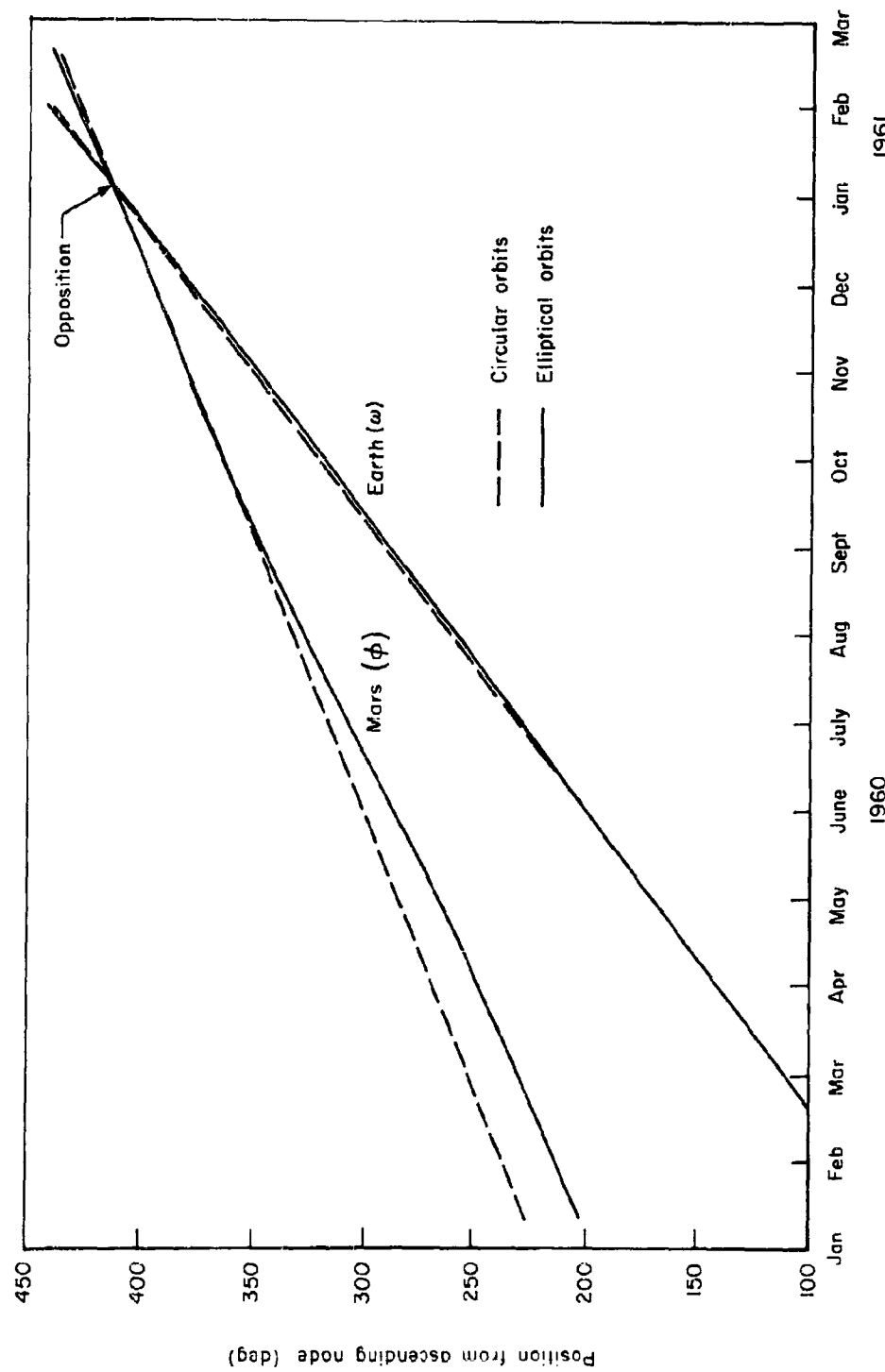


Fig.4—Position of Earth and Mars referred to ascending node

f. The graph obtained by plotting $T(A, C)$ vs θ was found to be well behaved, and as a consequence a technique like the Newton-Raphson method of successive approximations could be utilized to speed up the convergence of the solution $T(\theta) = 0$. (The dependence of T on θ arises after the solution of the time Eq. (1) for A has been carried out, so that A itself is a function of θ .)

Where one is not primarily interested in finding only optimal modes of transfer, but desires to get a fuller picture of the various trade-off values resulting from changes in initial conditions, one can neglect steps (d) - (f) and compute V_{CH} after step (c). In this way it is possible to see how the characteristic velocity varies with the transfer angle θ . Figure 5 presents a plot of V_{CH} against travel time for two chosen departure dates. Figure 6 presents the two components V_{CH_1} and V_{CH_2} of the total transfer requirement: V_{CH_1} denotes the characteristic velocity at launch, while V_{CH_2} refers to the landing portion.

The orientation of the transfer ellipse at the point of departure can be determined with the aid of the angle γ_1 which the initial velocity vector makes with the orbit of the Earth, as found from

$$\tan \gamma_1 = \sqrt{\frac{(2-L)A - 1}{AL}} \quad (13)$$

The calculated values of V_{CH_1} fix the magnitudes of the hyperbolic excess velocities which agreed closely with those of Fig. 1, Ref. 2, within the accuracy to which the data are presented.

As can be seen from the preceding paragraphs, the procedure of selecting optimal trajectories for the present two-dimensional models differs considerably from the one employed in Ref. 1. Whereas there, due to the absence

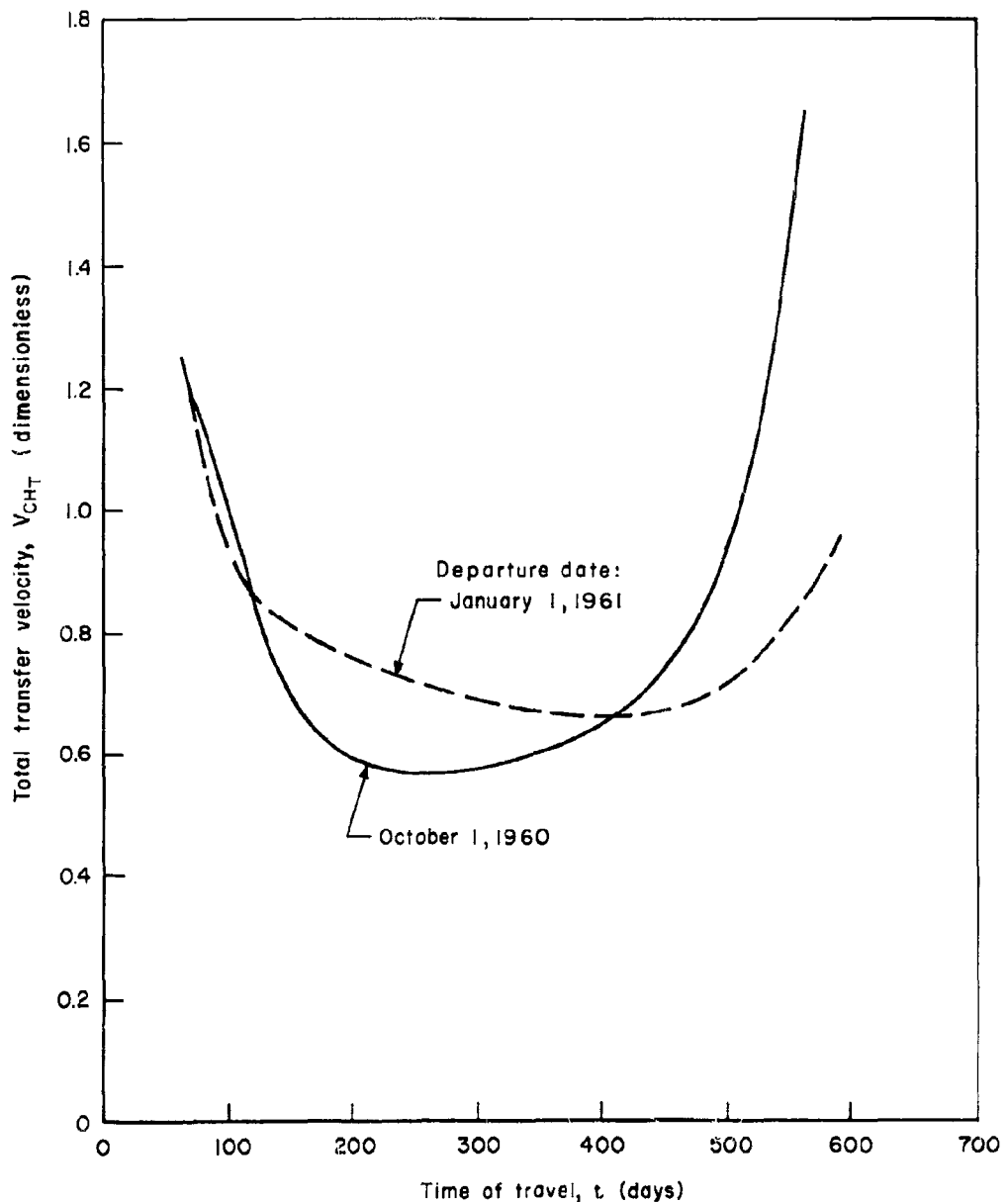


Fig. 5 — Coplanar characteristic - velocity variation

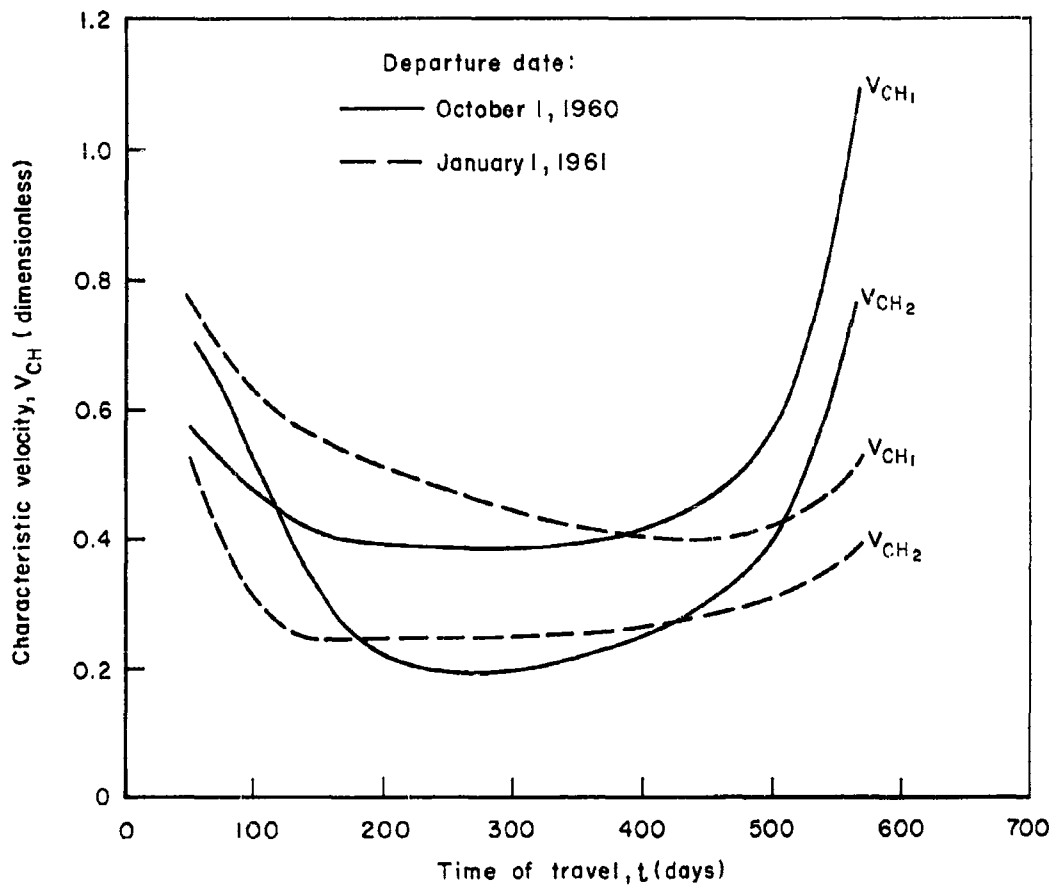


Fig.6—Coplanar departure and arrival velocity components

of a constraint on the travel time, all the ellipses possessing an $A > A_{\min}$ could be considered as suitable transfer orbits for any selected transfer angle θ , the present specification of an initial position of the target planet in general reduces this number to a single suitable ellipse. Furthermore, in Ref. 1 it was shown that there existed an optimal transfer ellipse for every selected angle of transfer. This is no longer true where the semi-major axis A is dependent on the transfer angle chosen through the time-constraint condition. Optimal modes of transfer can now occur only for discrete values of the transfer angle, or, what amounts to the same thing, transfer time.

For purposes of illustrating the method of solution in the coplanar case, a numerical example is worked out in Appendix A.

IV. THREE-DIMENSIONAL TRANSFERS WITH ECCENTRICITY

Up to now we have considered only circular coplanar planetary orbits. These restrictions on the orbits will now be lifted, thereby extending considerably the scope of the method developed. This will permit one to determine transfer trajectories between elliptic noncoplanar planetary orbits. The elliptic shape of the orbit of the destination planet will affect the manner of computing the travel time τ_o of that planet, while the presence of eccentricity in the initial orbit will change the form of the expression for the velocity increment to be added at departure, V_{CH_1} . In the majority of cases the eccentricities of the planetary orbits are rather small quantities. This makes it possible to simplify matters appreciably by retaining only linear terms in e in the series expansions of the planetary orbital elements. In particular, if one wants to be consistent in the order of magnitude of the perturbation terms retained for the case of travel from Earth to Mars, the fact that $e_M^2 \approx 0$ [e_E] allows one to ignore the eccentricity of the Earth's orbit when retaining only linear terms in the Martian elements. This section will thus be concerned with transfers from a point situated on an initial circular departure orbit to another point located on an inclined elliptic destination orbit.

The angle ψ measured counterclockwise from the ascending nodal line to the perihelion of the destination orbit will be assumed to be fixed in magnitude. For Mars, $\psi \approx 286$ deg. The geometry of the present model is shown in Figs. 7 and 8.

In three-dimensional maneuvers, the transfer plane will in general subtend an angle δ with the ecliptic and an angle ϵ with the orbital plane of

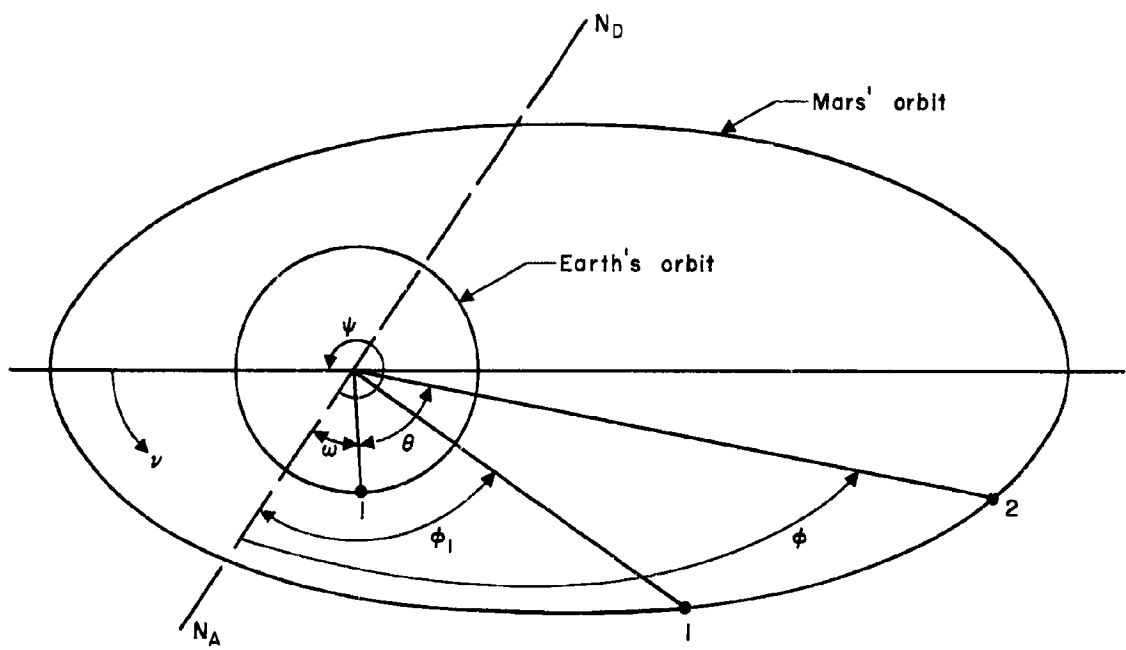


Fig.7—Parameters of Earth—Mars model

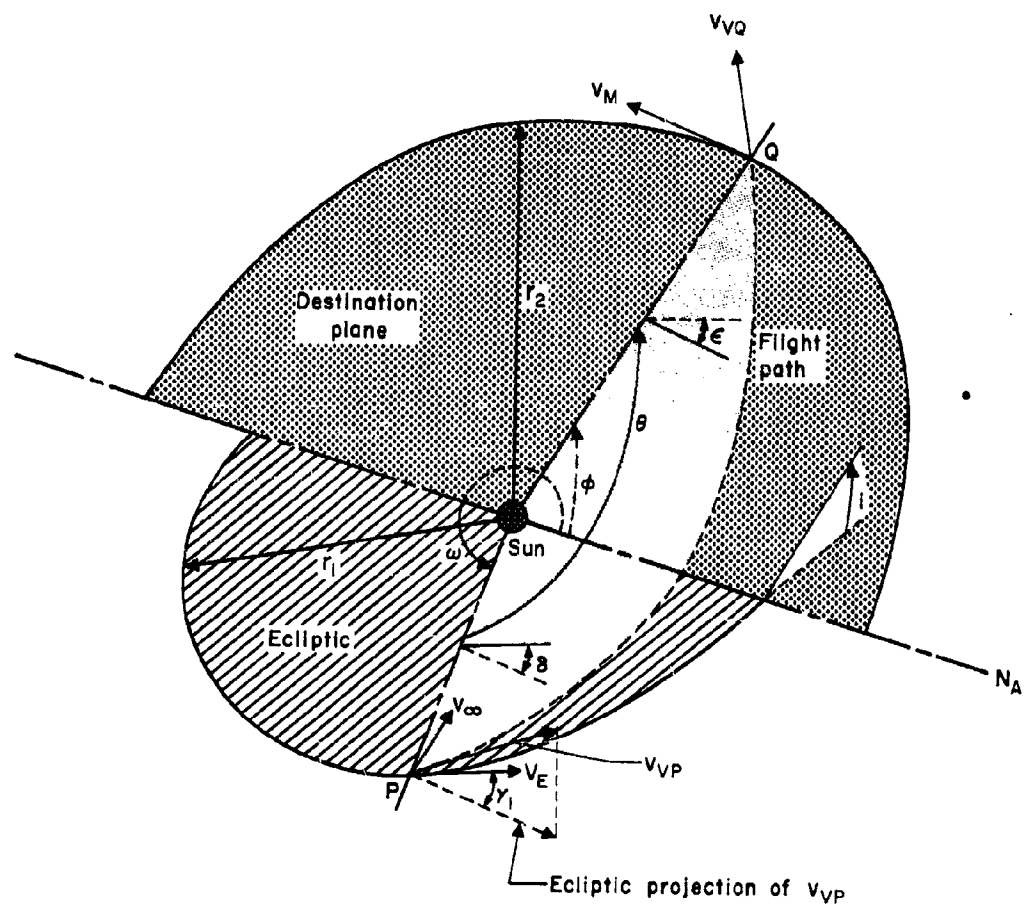


Fig.8—Orientation of orbital planes

the destination planet. From spherical trigonometry

$$\cos e = \sin i \sin \delta \cos \omega + \cos i \cos \delta \quad (14)$$

where i denotes the inclination of the destination plane with the ecliptic and ω denotes the location of the Earth referred to the ascending nodal line.

The transfer angle θ is now supplied by the expression

$$\cos \theta = \cos \omega \cos \phi + \sin \omega \sin \phi \cos i \quad (15)$$

in which ϕ denotes the angular position of the destination planet at the time of intercept, also measured from the ascending node.

In the present case, due to the small magnitude of the angle i , it is reasonable to make the approximation $\cos i \approx 1$, after which Eq. (15) becomes

$$\cos \theta = \cos (\phi - \omega) \quad (16)$$

and hence

$$\theta \pm 2\pi n = \phi - \omega \quad (17)$$

With the mean anomaly denoted by M , the dimensionless radial distance of Mars from the Sun becomes

$$\begin{aligned} \rho_M &= A_M \left[1 - e_M \cos M \right] + O \left[e_M^2 \right] \\ &= A_M \left[1 - e_M \cos N_M (\tau - \tau_p) \right] \end{aligned} \quad (18)$$

where

$$A_M = \frac{\rho_a + \rho_p}{2} = \rho_2 = \text{radius of approximated circular orbit}$$

τ_p = time of perihelion passage

r_a, r_p = radii at aphelion and perihelion, respectively

At time $\tau = \tau_1$, which corresponds to departure, the true anomaly of Mars, v_1 , is given by

$$v_1 = \theta_1 - \psi = M_1 + 2e_M \sin M_1 \quad (\text{Mod. } 2\pi) \quad (19)$$

where M_1 denotes the initial mean anomaly. If we follow the convention that positive angles are measured in the counterclockwise direction, a negative value for v_1 would imply that this angle is measured clockwise. In order to prevent this from happening, the restriction (Mod. 2π) should be understood to mean that an angle 2π has to be added to the computed value $\theta_1 - \psi$ whenever this quantity becomes negative. If this is done, then v_1 will always be located in the interval $0 - 2\pi$.

Equation (19) is basically Kepler's equation and can therefore be inverted to solve approximately for M_1

$$M_1 = v_1 - 2e_M \sin v_1 \quad (20)$$

Similarly, at arrival $\tau = \tau_2$ and $v_2 = \theta - \psi = (\omega - \psi) + \theta - 2\pi n$ ($n = 0, 1, 2, \dots$), so that for the case $n = 0$

$$M_2 = [(\omega - \psi) + \theta] - 2e_M \sin [(\omega - \psi) + \theta] \quad (21)$$

If we understand θ to denote the total angle covered by the radius vector from the Sun which rotates in a counterclockwise direction, starting from the ascending node of Mars and stopping at the point of intercept, after having passed in transit Mars' initial position θ_1 , it is clear that

$\theta = \theta_1 + \Delta\theta$. As used here, $\Delta\theta$ represents the angle covered by Mars during the transfer time and is a positive quantity. Adhering to the sign convention mentioned in connection with Eq. (19), we see that $v_2 > v_1$ and that, in addition, v_2 can exceed 2π in magnitude.

The time of transit from the initial point P to the final point Q is readily available from the relation

$$\tau_{PKQ} = \frac{M_2 - M_1}{N_M} \quad (22)$$

where

$$M_2 > M_1$$

The letter X in the subscript stands for any one of the intermediate stations F or F^* discussed earlier.

The inclination δ of the transfer plane is obtained from the relation

$$\sin \delta = \sin i \frac{\sin \theta}{\sin \theta} \quad (23)$$

If we refer to Eq. (17), Eq. (23) becomes

$$\sin \delta = \sin i \frac{\sin (\theta + \omega)}{\sin \theta} \quad (24)$$

At any point along its orbit, the velocity components of Mars are given approximately by the expressions

$$\begin{aligned} v_{rM} &= \dot{r}_M = N_M \rho_2 e_M \sin M \\ v_{\theta M} &= (\dot{\theta} \rho)_M = N_M \rho_2 (1 + e_M \cos M) \end{aligned} \quad (25)$$

The above relations are used to obtain a new expression for the characteristic transfer velocity, as shown in Eq. (26).

$$\begin{aligned} v_{CH} = & \left\{ 3 - \frac{1}{A} - 2\sqrt{\frac{L}{\rho_2}} \cos \delta + K_3 \right\}^{1/2} + \frac{1}{\sqrt{\rho_2}} \left\{ 3 - \frac{\rho_2}{A} - 2\sqrt{\frac{L}{\rho_2}} \cos \epsilon \right. \\ & \left. + 4e_M \cos M_2 \left[1 - \sqrt{\frac{L}{\rho_2}} \cos \epsilon \right] - 2e_M \sin M_2 \sqrt{2 - \frac{L}{\rho_2} - \frac{\rho_2}{A} + \rho_2 K_4} \right\}^{1/2} \end{aligned} \quad (26)$$

(A derivation of Eq. (26) is given in Appendix B.)

As is to be expected, Eq. (26) becomes identical with Eq. (5) if we set

$$e_M = \epsilon = \delta = 0$$

The steps necessary for the solution of the present case are not too different from the ones described in the coplanar case. The main difference arises in the computation of the time of transfer, t_{PQ} .

At the time of departure, the initial angular position of the Earth, ω , and of Mars, θ_1 , are known quantities. If, as before, a transfer angle θ is chosen, one can compute the mean anomalies M_1 and M_2 from Eqs. (20) and (21).

Similarly, with M_2 known, ρ_M can be obtained from Eq. (18).

With the above information we can now find the length of the chord joining points P and Q from the relation

$$c^2 = 1 + \rho_{M_2}^2 - 2\rho_{M_2} \cos \theta \quad (27)$$

where

ρ_{M_2} = magnitude of ρ_M when $M = M_2$ in Eq. (18)

Having now obtained the values of τ and C , we can continue with the computational procedure outlined in the previous section. Equations (14) and (24) show that for given fixed values of ω , θ , and i , after account is taken of Eq. (27), the angles δ and ϵ will depend only on the chord C . From this we conclude that the condition of optimality, Eq. (12), is also applicable in the present case, provided Eq. (22) is employed to compute the time τ_0 appearing in Eq. (9).

The expression for the inclination γ_1 of the departure velocity vector remains unaffected by the eccentricity e_M and can be used in its initial form.

It was noted that for the two-dimensional circular case the only input information needed was the initial longitude difference of the two planets. In the present case, their actual positions in orbit, ω and θ_1 , have to be specified. In all other respects the method of carrying out the solution remains unchanged.

Figure 9 shows a plot of V_{CH} vs time for the three-dimensional model of the planetary system. In each case, departure was assumed to take place on October 1, 1960.

It can be seen that the curves consist of two separate, parabolically shaped branches. One branch corresponds to values of the travel angle $\theta < 180$ deg, while the other refers to $\theta > 180$ deg. Due to the inherent geometry of inclined planes, transfers through angles in the immediate vicinity of 180 deg are, in general, impossible except for transfer trajectories that originate at the nodal line.

Two regions of minimal transfer velocity are now found for each selected departure date, separated from each other by the narrow belt $\theta \sim 180$ deg. The value of $V_{CH \min}$, on which the optimization procedure outlined before

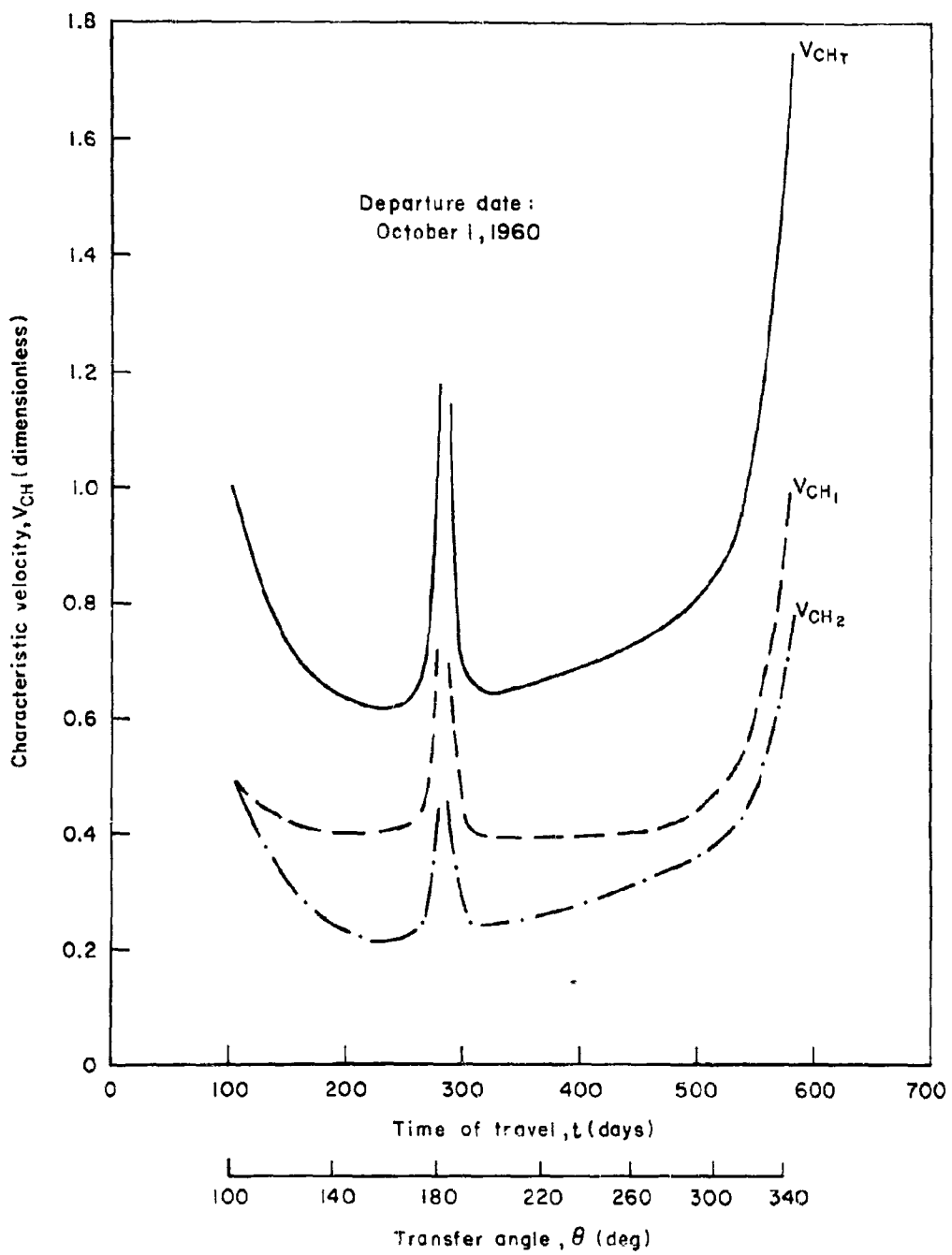


Fig.9—Three-dimensional characteristic-velocity variation

will converge, will depend on the initial value of θ selected to start the iteration. The $V_{CH \min}$ for long-period transfers will be found if one starts the iteration with a value of $\theta > 180$ deg, while the short transfer time $V_{CH \min}$ is reached upon starting out with a $\theta < 180$ deg. An idea of the change in orientation of the departure velocity vector as the time of transfer, as well as the transfer angle, is increased can be gained from Fig. 10. This figure presents the two angles δ and γ_1 plotted against transfer time τ .

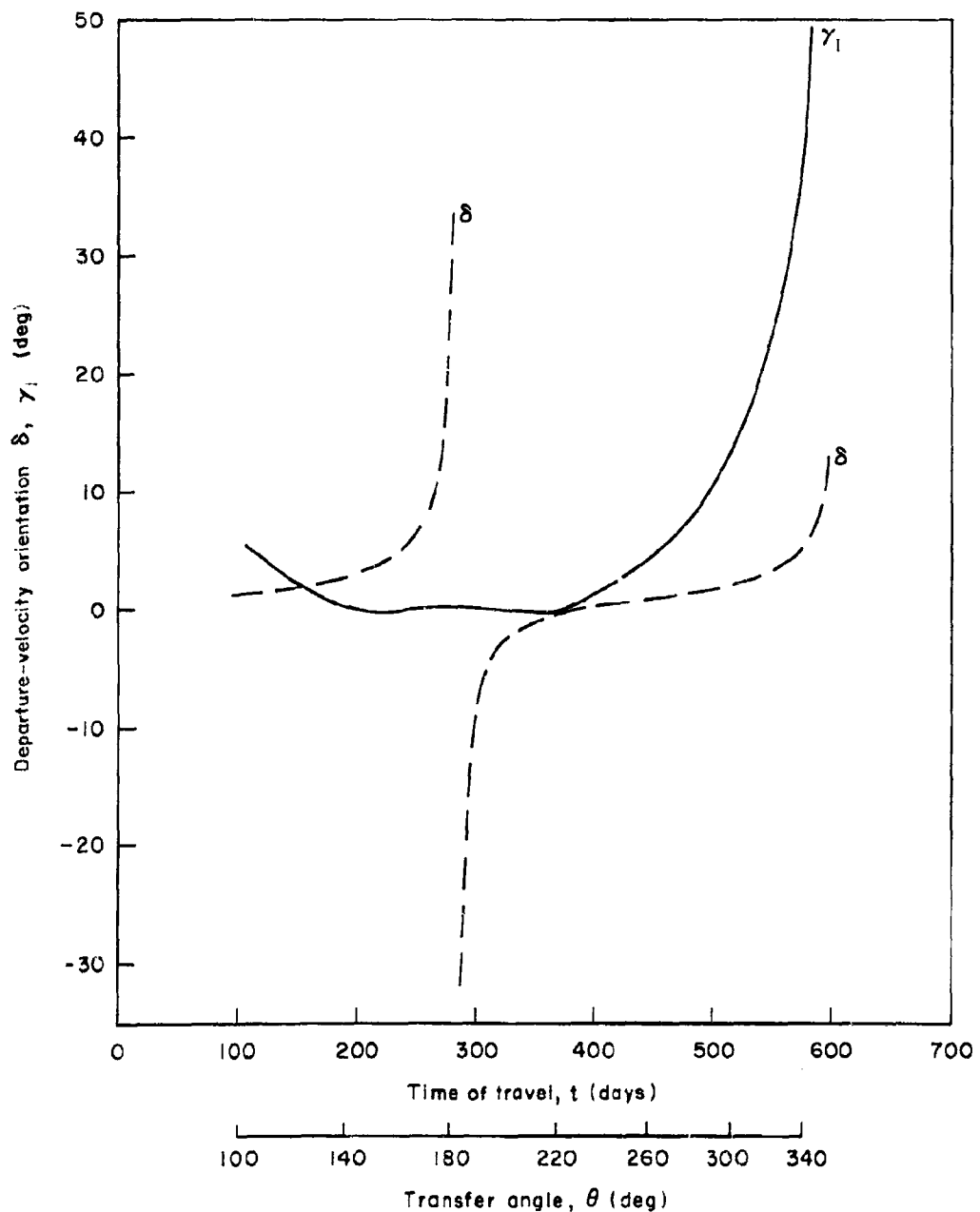


Fig.10—Variation of δ and γ_1 with flight time

Appendix A

NUMERICAL EXAMPLE

A numerical example is worked out in detail in this appendix to illustrate the general method of solution.

For the sake of convenience, a two-dimensional circular planetary model has been selected, with the following input data:

θ_0 = initial longitude difference = 30 deg
(Mars leading the Earth)

θ = transfer angle = 140 deg

r_1 = 1.0 = radius at point of departure P

r_2 = 1.523 = radius at point of arrival Q

From the above data, the chord joining points P and Q is computed to be

$$C = \left[1 + 1.523^2 - 2 \cdot 1.523 \cos 140^\circ \right]^{1/2} = 2.3776$$

With the dimensionless mean angular velocity of Mars given by

$$N_M = \frac{v_M}{v_E} \cdot \frac{r_1}{r_2} = \frac{15.0}{18.5} \cdot \frac{1}{1.523} = 0.5324$$

we find that the time required by Mars to traverse and angle $\theta - \theta_0$ is

$$\tau_0 = \frac{\theta - \theta_0}{N_M} = \frac{110}{57.296 \cdot 0.5324} = 3.6061$$

The value of the minimum semimajor axis A_m for the present case is

$$A_m = \frac{1 + 1.523 + 2.3776}{4} = 1.22515$$

The example chosen here happens to have a value of the transfer angle $\theta < \pi$, so that, in accordance with the discussion presented in connection

with Fig. 3, the appropriate expression for the time of transit would have to be selected from Eqs. (1a) or (1b) (τ_{PQ} and τ_{PF}^*Q). The selection can be narrowed down further if we determine whether τ_o is greater or smaller than the value of τ at $A = A_m$, at which point $\tau_{PQ} = \tau_{PF}^*Q$.

$$\tau_{PQ} = A^{3/2} \left[(\alpha - \sin \alpha) - (\beta - \sin \beta) \right]$$

For the present case

$$S = \frac{1 + \rho_2 + C}{2} = 2.4503$$

$$S - C = 0.0727$$

thus

$$\alpha_m = 2 \sin^{-1} \sqrt{\frac{S}{2A_m}} = 2 \sin^{-1} \sqrt{\frac{2.4503}{2.4503}} = 2 \sin^{-1} 1 = \pi$$

$$\beta_m = 2 \sin^{-1} \sqrt{\frac{S - C}{2A_m}} = 2 \sin^{-1} \sqrt{\frac{0.0727}{2.4503}} = 0.3462$$

$$\sin \alpha_m = 0 \quad \sin \beta_m = 0.3393$$

$$\tau_m = (1.22515)^{3/2} \left[3.1416 - 0.3462 + 0.3393 \right] = 4.251$$

Now that we have determined that $\tau_o < \tau_m$, we conclude, with the aid of Fig. 3, that the appropriate time expression to be used in the present case is the τ_{PQ} relation; the vacant focus of the proper transfer ellipse will be located on the L_+ branch of the curve of Fig. 2.

What remains to be done now is to solve from the expression for τ_{PQ} , Eq. (1a), for the correct value of A which satisfies the condition

$$\tau_{PQ} = \tau_o = 3.6061$$

This will be accomplished by a trial-and-error procedure which can be suitably adapted to locate the proper root very quickly.

Let us start out with a first guess for A.

Guess 1: $A = 1.32$

$$A^{3/2} = 1.5167$$

$$\alpha = 2 \sin^{-1} \sqrt{\frac{2.4503}{2.64}} = 2 \sin^{-1} 0.9634 = 2.5988$$

$$\beta = 2 \sin^{-1} \sqrt{\frac{0.0727}{2.64}} = 2 \sin^{-1} 0.16595 = 0.3334$$

$$\sin \alpha = 0.51654 \quad \sin \beta = 0.32726$$

and

$$\tau = 1.5167 [2.5988 - 0.51654 - 0.3334 + 0.32726] = 3.1489$$

Since this value is smaller than the desired one, we would have to take a smaller value of A as a second guess. In order to come up with an intelligent second guess for A, we can make use of the shape of the τ vs A curve of Fig. 3, in particular that portion in the neighborhood of the point (τ_m, A_m) . If we draw a curve between the latter point and the point $(3.1489, 1.32)$ as shown in Fig. 11, such that $d\tau/dA = \infty$ at A_m , we find that at a value of $\tau = 3.6$, $A \approx 1.25$.

Accordingly we let our second guess be

Guess 2: $A = 1.25$

$$A^{3/2} = 1.3975$$

$$\alpha = 2 \sin^{-1} \sqrt{\frac{2.4503}{2.5}} = \sin^{-1} 0.99001 = 2.8588$$

$$\beta = 2 \sin^{-1} \sqrt{\frac{0.0727}{2.5}} = \sin^{-1} 0.17053 = 0.34276$$

$$\sin \alpha = 0.2867 \quad \sin \beta = 0.33608$$

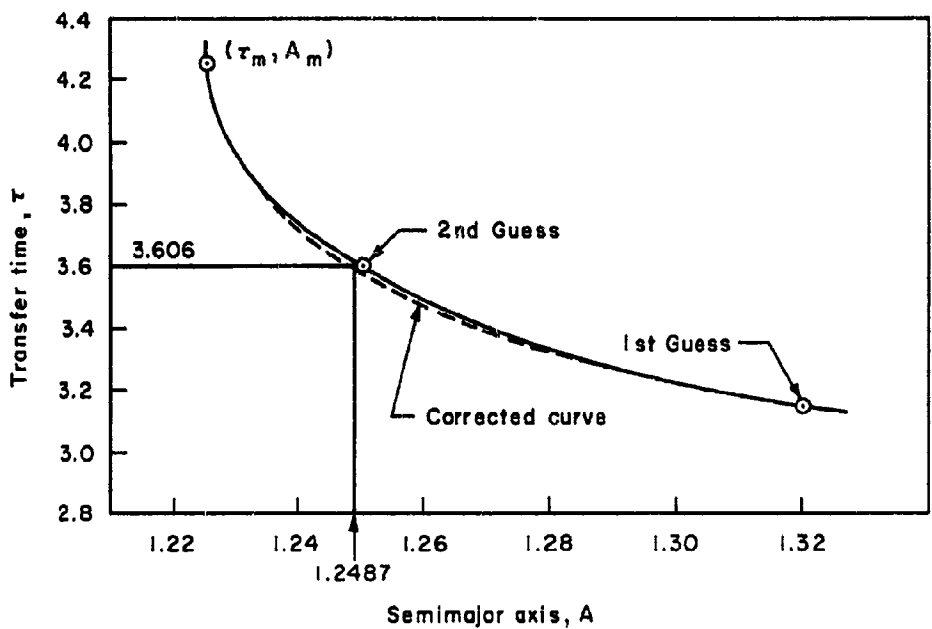


Fig. II—Approximated τ vs A curve for graphical iteration

and

$$\tau = 1.3975 \left[2.8588 - 0.2867 - 0.34276 + 0.33608 \right] = 3.5851$$

Plotting a corrected curve in Fig. 11 through the three known points, we find that a third guess should be around $A = 1.2485$.

Guess 3: $A = 1.2485$

Repeating the calculations performed before, we arrive at a value for time τ of 3.613. To the degree of accuracy needed, a satisfactory solution can be taken to be a value of $A = 1.2487$.

The total characteristic transfer velocity can now be computed from Eq. (5). First we shall compute the constants K_3 and K_4 appearing there:

$$K_3 = \frac{2\mu_E}{R_E} \frac{r_1}{\mu} = \frac{v_{E \text{ esc}}^2}{v_1^2} = \left(\frac{6.95 \text{ mi/sec}}{18.5 \text{ mi/sec}} \right)^2 = 0.1412$$

$$K_4 = \frac{2\mu_M}{R_M} \frac{r_1}{\mu} = \frac{v_{M \text{ esc}}^2}{v_1^2} = \left(\frac{3.1 \text{ mi/sec}}{18.5 \text{ mi/sec}} \right)^2 = 0.0281$$

where $v_{E \text{ esc}}$ and $v_{M \text{ esc}}$ are the surface escape velocities for Earth and Mars, respectively.

The magnitude of the semilatus rectum L , calculated from Eq. (2a), is found to be $L = 1.187$.

With the above values, Eq. (5) gives

$$\begin{aligned} v_{CH_T} &= \left\{ 3 - \frac{1}{1.2487} - 2\sqrt{1.187 + 0.1412} \right\}^{1/2} \\ &\quad + \frac{1}{1.2341} \left\{ 3 - \frac{1.523}{1.2487} - 2\sqrt{\frac{1.187}{1.523} + 1.523 \cdot 0.0281} \right\}^{1/2} \\ &= 0.4020 + 0.1944 = 0.5964 \end{aligned}$$

Since the two members of the above sum supply the velocity requirements at departure and arrival, respectively, we find in dimensional form

$$v_{CH_T} = 0.5964 \cdot 97,680 = 58,256 \text{ ft/sec}$$

$$v_{CH_1} = 0.4020 \cdot 97,680 = 39,267 \text{ ft/sec}$$

$$v_{CH_2} = 0.1944 \cdot 97,680 = 18,989 \text{ ft/sec}$$

The angle γ_1 which the departure velocity vector subtends with the Earth's orbital path is found to be

$$\gamma_1 = \tan^{-1} \sqrt{\frac{(2 - L) A - 1}{AL}} = \tan^{-1} 0.10123 = 5^{\circ}47'$$

This completes the illustrative computation for the two-dimensional example chosen. The same basic scheme can, of course, be followed also in the more complicated case of three-dimensional circular-to-elliptic transfers, provided the time τ_0 is properly evaluated and the radius r_{M_2} has been determined in accordance with the method outlined previously.

Appendix B

CHARACTERISTIC TRANSFER VELOCITY IN THREE DIMENSIONS

The velocity components of a body moving along a conic section, projected onto the radial and transverse directions, were given by Eqs. (2.1.2) and (2.1.3) of Ref. 1. Applying these expressions to the planet Mars we have

$$v_{r_M} = (\dot{r})_M = \left[\mu \frac{2r_M - l_M}{r_M^2} - \frac{\mu}{r_2} \right]^{1/2} \quad (B.1)$$
$$v_\theta_M = (r\dot{\theta})_M = \sqrt{\frac{\mu l_M}{r_M}}$$

In the above relations, r_M denotes the instantaneous radial distance of Mars while r_2 denotes the average radius of the orbit which, to first-order terms in e_M , equals the semimajor axis a_M . The term l_M is the semilatus rectum of the Martian orbit.

If one employs the relations

$$r_M = r_2 \left[1 - e_M \cos M \right] \quad (B.2)$$
$$l_M = r_2 \left[1 + e_M^2 \right]$$

differentiates the first to obtain \dot{r}_M and substitutes both into the v_θ expression of Eq. (B.1), one finds that for small values of e_M

$$v_r = \sqrt{\frac{\mu}{r_2}} e_M \sin M \quad (B.3)$$
$$v_\theta = \sqrt{\frac{\mu}{r_2}} (1 + e_M \cos M)$$

Denoting by v_{RQ} the velocity of the vehicle relative to a nonattracting planet located at point Q, we can write

$$v_{RQ}^2 = \left[(\dot{r})_M - v_{r_M} \right]^2 + (r\dot{\theta})_M^2 \sin^2 \epsilon + \left[(r\dot{\theta})_M \cos \epsilon - v_{\theta_M} \right]^2 \quad (B.4)$$

where $(\dot{r})_M$ and $(r\dot{\theta})_M$ are the heliocentric velocity components of the vehicle in its own plane of motion, evaluated at the point of intersection of the transfer plane with the Martian orbit, and are given by

$$\begin{aligned} (\dot{r})_M &= \left[\mu \frac{2r_M - 1}{r_M^2} - \frac{\mu}{a} \right]^{1/2} \\ (r\dot{\theta})_M &= \sqrt{\frac{\mu l}{r_M}} \end{aligned} \quad (B.5)$$

The symbols l and a refer respectively to the semilatus rectum and semi-major axis of the transfer ellipse. Equations (B.3) and (B.5) can now be substituted into Eq. (B.4). After expanding some of the terms, retaining only linear terms in e_M , and combining them appropriately, one is led eventually to the following nondimensionalized relation for v_{RQ}^2

$$\begin{aligned} v_{RQ}^2 &= \frac{1}{\rho_2} \left\{ 3 - \frac{\rho_2}{A} - 2 \sqrt{\frac{L}{\rho_2}} \cos \epsilon + 4e_M \cos M_2 \left(1 - \sqrt{\frac{L}{\rho_2}} \cos \epsilon \right) \right. \\ &\quad \left. - 2e_M \sin M_2 \sqrt{2 - \frac{L}{\rho_2} - \frac{\rho_2}{A}} \right\} \end{aligned} \quad (B.6)$$

For the departure portion of the transfer, the angle δ takes the place of the angle ϵ used above. The relative departure velocity increment is

$$v_{RP}^2 = \left\{ 3 - \frac{l}{A} - 2 \sqrt{L} \cos \delta \right\} \quad (B.7)$$

Upon inclusion of the planetocentric gravitational take-off and landing requirements through the relations

$$v_{T.O}^2 = v_{CH_1}^2 = v_{RP}^2 + \frac{2\mu_E}{R_E} \quad (B.8)$$

and

$$v_{LAND}^2 = v_{CH_2}^2 = v_{RQ}^2 + \frac{2\mu_M}{R_M} \quad (B.9)$$

one finds for the total characteristic surface-to-surface transfer velocity

$$v_{CH} = v_{CH_1} + v_{CH_2}, \text{ the relation shown in Eq. (26).}$$

REFERENCES

1. Battin, R. H., "The Determination of Round-Trip Planetary Reconnaissance Trajectories," J. Aero/Space Sci., Vol. 25, No. 9, September 1959.
2. Breakwell, J. V., R. W. Gillespie, and S. Ross, Researches in Interplanetary Transfer, ARS Preprint 954-59, 14th Annual Meeting, November 16, 1959.
3. Whittaker, E. T., A Treatise on the Analytical Dynamics of Particles and Rigid Bodies, 4th ed., Dover Publications, Inc., New York, 1937.